Exoplanet Detection via Transit Photometry with the Great Basin Observatory

University of Nevada, Reno

March 29, 2019

Abstract

Exoplanet detection via transit photometry has blossomed into one of the most fruitful fields in all of physics in the last decade with NASA missions like *Kepler*. An exoplanet transit refers to the event where a planet in orbit around a host star passes between the line of sight of an observer and the host star. If the brightness of host star were to be monitored during a transit event, such as with a light curve (a plot of the star's brightness throughout time), the observer would notice a decrease in the host star's brightness due to the interference of the planet. Through light curve generation from an exoplanetary transit, estimates of planet parameters like radius and semimajor axis can be obtained. We conducted transit photometry on the star Kepler-17, known host to exoplanet Kepler-17b, on June 26, 2018 using the Great Basin Observatory in an effort to perform the one of the first exoplanet detections in the telescope's 2-year history. We also sought to gauge the lower limits of host star brightness for which the 0.7-meter telescope retains sensitivity and establish a transit depth threshold for detection confidence. We present evidence for detection of Kepler-17b, estimates of its radius, semimajor axis and orbital period, as well as a transit depth minimum for GBO detection.

Contents

1   Introduction

The first sign of convincing evidence for planets existing beyond our solar system occurred in 1992 with radio pulsar timing [1]. Exoplanet detection using transit photometry first occurred over a decade later in 2003. Since then, the transit method has played the dominant role in the over 3,800 confirmed exoplanets that exist today [2]. One of the most desirable attributes of this approach is its ability to lead directly to an estimation of the planet's radius. From the planet radius measurements to date, we find that the vast majority of exoplanets are "Hot Jupiters" (large planets orbiting close to their host star), which is far different from the makeup of our solar system.

When an outside body passes between the line of sight of a light source and an observer, the event is called a transit. The most well-known event of this sort is when the moon passes between the Earth and the Sun in a solar eclipse. During the transit time, the light received from the source decreases due to the outside body's interference, just as the sky darkens during a solar eclipse. In the discovery of exoplanets, we continually observe stars to search for repeating dips in light that would occur if an orbiting planet periodically crossed the path between the Earth and the host star. Although most exoplanet detections using the transit method have been with space-based telescopes like NASA's *Kepler*, detection with ground-based telescopes like the Great Basin Observatory (GBO) is also possible. Here we present our detection of exoplanet Kepler-17b along with estimates for the planet's parameters. Moreover, we discuss the GBO's planet detection sensitivity using the transit method.

The structure of this paper is as follows. In Sec. 2 we provide an outline of the theory behind exoplanet observations using transit timing. In Sec. 3 we discuss our observations with the GBO and the planet Kepler-17b. An outline of the data analysis procedure is provided in Sec. 4 while results of our observations are provided in Sec. 5. Lastly, we include a discussion of results in Sec. 6 and a single appendix that discusses the GBO.

2 Theory

Extraction of planet parameters from transit observations comes entirely from analysis of light curves. Among the planet parameters linked to light curves from transit observations are the planet radius R_{pl}, semi-major axis a, impact parameter b, inclination i and orbital period P. When a planet of radius R_{pl} is directly in the observer line of sight with the host star of radius R_*, the difference in normalized stellar brightness ΔL is

$$\Delta L = \left(\frac{R_{pl}}{R_*}\right)^2. \tag{1}$$

If the radius of the host star is known, the radius of the exoplanet immediately follows. The dip deviates from above in times when the planet and star are only partially overlapping. Expressions for the received stellar flux during these times is provided in Ref. 3. Moreover, this assumes that the host star contains a uniformly bright surface therefore neglecting limb darkening corrections[1]. A planet's transit of its host star is split into 4 contacts (t_1, t_2, t_3, and t_4, each time the planetary disk is tangent to the stellar disk) and a midpoint t_c as shown in Fig. 1. The *ingress* of a transit corresponds to the time from t_1 to t_2 while the *egress* is from t_3 to t_4. Utilizing the same approach as Ref. 3, we will establish characteristic timescales τ and T, both dependent on the times when each of the transit stages occur. Expression for planet parameters will be given in terms of these timescales,

$$\tau = \frac{t_3+t_4}{2} - \frac{t_1+t_2}{2} \tag{2}$$

$$T = t_2 - t_1 = t_4 - t_3 \tag{3}$$

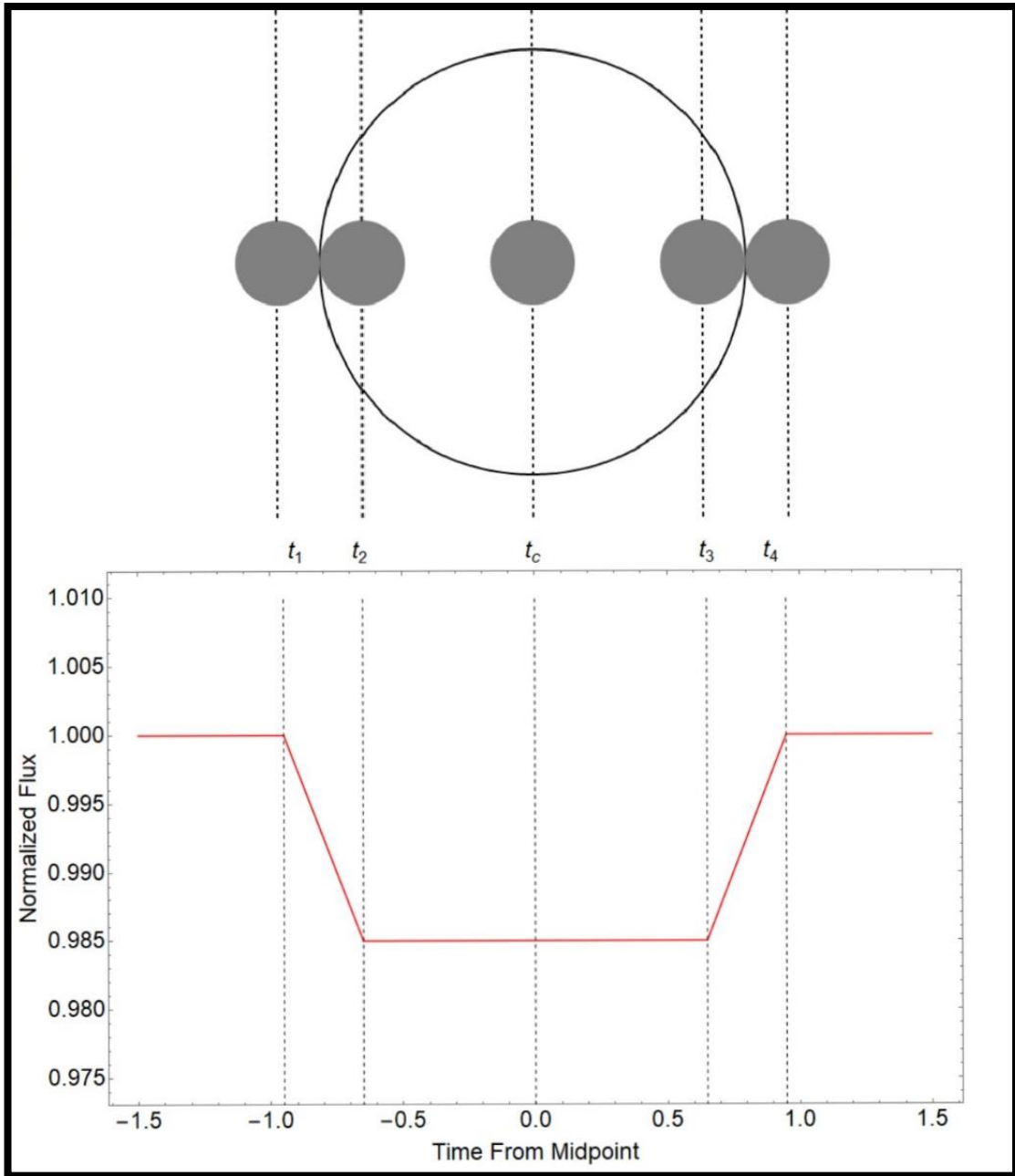[1] Limb darkening corrections are considered extensively in Ref. 1.

Figure 1: Illustration depicting how the depth of the light curve corresponds to the stage of the transit. *Stages:* (t_1) First Contact (Ingress Exterior), (t_2) Second Contact (Ingress Interior), (t_c) Midpoint, (t_4) Third Contact (Egress Interior), and (t_5) Fourth Contact (Egress Exterior).

These characteristic times are linked to the radius ratio $r = R_{pl}/R_*$ and impact parameter b by (see e.g., Ref. 3)

$$\tau = 2\tau_0\sqrt{1 - b^2} + O(r^2) \qquad (4)$$

$$T = 2\tau_0\frac{r}{\sqrt{1-b^2}} + O(r^3) \qquad (5)$$

where, if we assume an eccentricity of zero (i.e., a circular orbit), $\tau_0 = R_*P/2\pi a$ and $b = a\cos i/R_*$. The second and third order corrections $O(r^2)$ and $O(r^3)$ in Eqs. (4) and (5) can be ignored for simplicity. Using these characteristic time scales, a piecewise linear light curve model for the normalized observed stellar brightness L can be established

$$L(t) = \begin{cases} 1 - \Delta L & |t-t_c| \leq T/2 - \tau/2 \\ 1 - \Delta L + (\Delta L/\tau) \times (|t - t_c| - T/2 + \tau/2) & T/2 - \tau/2 < |t-t_c| \leq T/2 + \tau/2 \\ 1 & |t-t_c| \geq T/2 + \tau/2 \end{cases} \qquad (6)$$

This piecewise linear model mirrors the model developed in Ref. 3. The benefit of this linear model is the ability to relate the characteristic timescales τ and T to planet parameters b and τ_0 (see e.g., [3]):

$$b^2 = \left(\frac{a\cos i}{R_*}\right)^2 = 1 - r\frac{T}{\tau} \qquad (7)$$

$$\tau_0^2 = \left(\frac{R_*P}{2\pi a}\right)^2 = \frac{T\tau}{4r}. \qquad (8)$$

We can also obtain an approximation for the planet period P rather trivially by observing consecutive transits. Then, since the planet's mass M_{pl} is generally a few orders of magnitude lower than the mass of the host star M_*, Kepler's Third Law can provide an approximation for the semi-major axis

$$a^3 \approx \left(\frac{GM_*}{4\pi^2}\right)P^2. \qquad (9)$$

4

3 Observations

a. Utilizing the GBO

The Great Basin Observatory has a 0.7-meter aperture telescope with a 4096×4096-pixel charge-coupled device (CCD). On board the GBO are the standard BVRI filters for photometry and various other filters for atmospheric and astronomical observations. The observations on Kepler-17b were done with a CCD temperature of $-25°C$ and using a pixel binning of two, reducing the effective CCD size to 2048×2048. The R-band filter was utilized, covering wavelengths from 550nm to 700nm. We took 165 images each with exposure times of 40 seconds prior to experiencing cloud obstruction and ending operations before observing a complete transit.

The GBO also has an archive of bias, dark and flat calibration frames for various exposure times, filters and CCD temperatures. Bias frames are zero-time exposure images taken with the shutter closed and reduce CCD read noise when subtracted out of the raw images. Dark frames are images taken at the same temperature and exposure time as the normal images but without light reaching the sensor. Since some pixels can still contain a signal even when no light has reached it, dark frames zero the CCD pixels when subtracted out. A flat frame is a picture taken at the same exposure time and with the same filter as the raw image but focused on an evenly illuminated surface. The flats serve to correct optical imperfections like vignetting or dust interference.

b. Kepler-17b

The host star of the planet we observed, Kepler-17, is a 14.0 magnitude type G star approximately 800 parsecs away from Earth [4]. The star has a radius of $1.05R_{sun}$ and a mass of $1.16M_{sun}$ [4]. Kepler-17b is the lone planet in that system with an accepted radius of $1.312R_{Jup}$ and mass of $2.45M_{Jup}$ [4]. With an orbital period of under two days, Kepler-17b is

categorized as a Hot Jupiter. The size and period of this planet make it ideal for detection via the transit method since transits will be frequent and the luminosity drop of the host star will be much more noticeable compared to an Earth-sized planet.

Expected transit times for Kepler-17b were generated using the NASA exoplanet archive and specifying our observing location[2] [2]. Between June 20, 2018 and July 10, 2018, there were 5 transits predicted to be in the line of sight of the GBO, with all of them occurring during observable hours of the night [2].

4   Analysis

a. Data Reduction

To optimize pixel quality, the raw images from the GBO undergo a multi-step step data reduction process. First, master calibration frames are created by generating images of the median pixel value from each of the original calibration images. The master bias is subtracted from the raw images to eliminate CCD bias voltage contributions. Then, the master bias is subtracted from the master dark and the subsequent dark image is subtracted from the raw images to eliminate hot pixels. Each image is divided by the master flat frame to minimize the contribution of dust in the telescope and vignetting. The difference between raw and calibrated images is shown in Fig. 2. Lastly, calibrated images were aligned using Kepler-17b and 4 other star positions in each image. These calibration and alignment processes were done using AstroImageJ.

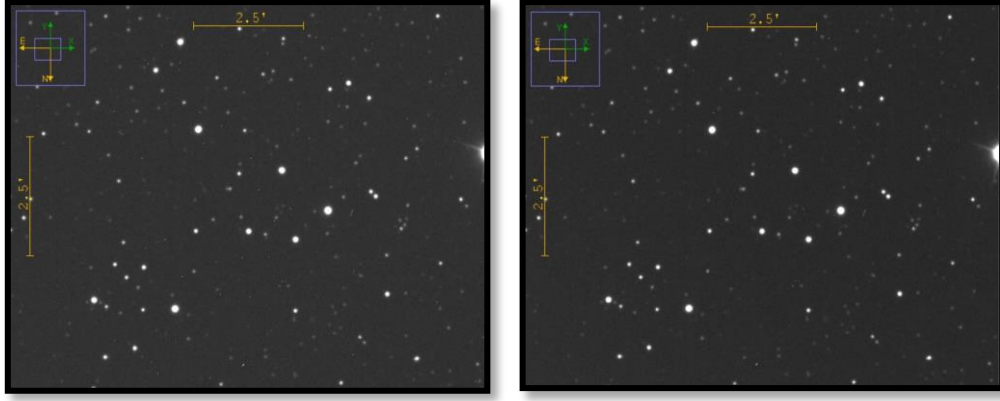[2] The Great Basin Observatory is located at 39° North, 114° West.

Figure 2: Results of data reduction process on the raw GBO images. (Left) Unprocessed image taken by the GBO telescope. (Right) Calibrated GBO image with bias and dark subtracted and flat divided.
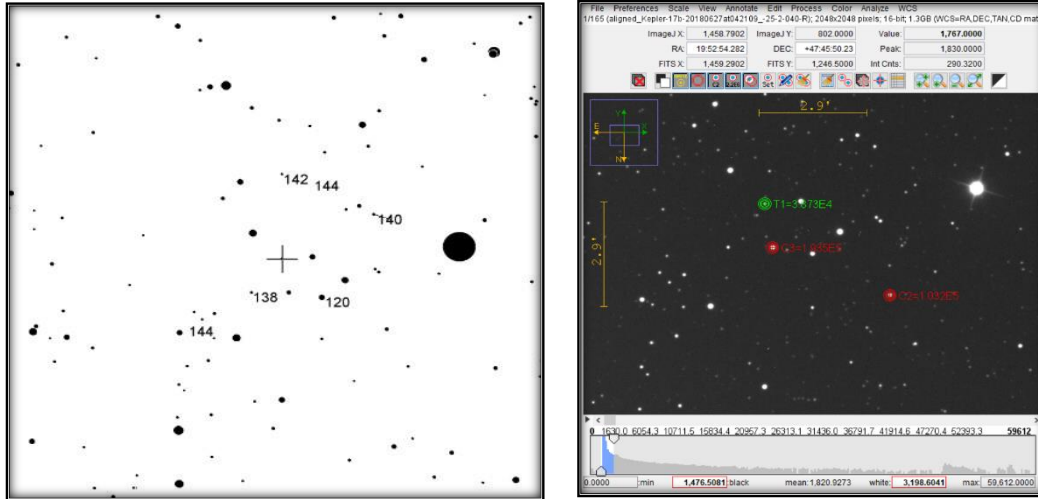

Figure 3: Selection process of host star (T1) and comparison stars (C2, C3). (Left) Finder chart for locating host star. (Right) Selection of host star and 2 comparison stars (C2, C3) in calibrated and aligned image set for relative flux analysis.

b. Light Curve Generation

Relative flux data used for light curve generation was gathered using the multi-aperture setting in AstroImageJ. In this process, the target star is chosen along with comparison stars in the region as shown in Fig. 3. To calculate the relative flux, the number of counts received by the target star is divided by the sum of the pixel counts received by the

comparison stars. It is important to choose stars that exhibit a constant flux throughout the transit duration since these stars are used to determine if the target star's brightness changes. Using a variable star for comparison can skew results.

Each relative flux was normalized. For Kepler-17, the relative flux was normalized using the first 30 images, when Kepler-17b was in a pre-transit state. The comparison stars were also normalized using the first 30 images for consistency. After generating normalized flux data, we performed light curve generation and planet parameter calculations.

5   Results

The nearly complete transit of Kepler-17b observed on June 26, 2018 is shown in Fig. 4. The normalized flux exhibits a clear drop below the pre-transit trend starting at JD-2400000 time 58296.710 and throughout the rest of the observing window. To verify the reliability of the comparison stars, light curves were generated for each using their normalized flux as shown in Fig 5. Each comparison star exhibited a constant normalized flux throughout the observation window as desired. The comparison of the Kepler-17b light curve to those of the comparison stars confirms the exoplanet detection. The light curves for Kepler-17b and the 2 comparison stars are plotted together in Fig. 6.
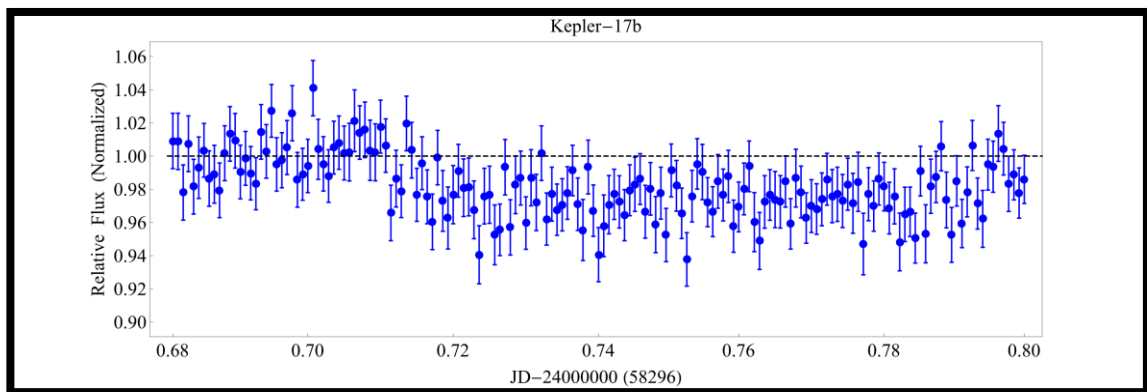
Figure 4: Kepler-17 normalized relative flux light curve.

Using the light curves for the comparison stars, one may establish a transit depth limit for exoplanet detection with the GBO (the minimum drop in brightness needed in a light curve to be confident that the drop was not due to random star brightness fluctuations) and establish the statistical significance of detection. For this we treat the normalized relative flux of the reference stars for the 40 second exposures as Gaussian random variables[3] with mean equal to 1 and standard deviation calculated to be 0.00694 for star C2 and 0.00695 for star C3. Then one can be 90% confident that each observation, given that there is no transit occurring, will remain within 1.14% of mean normalized relative flux. This establishes a minimum transit depth threshold for which the GBO will be able to detect, that is, brightness drops larger than 1.14% are detectable by the GBO. In general, the depth of detectable transits may vary with
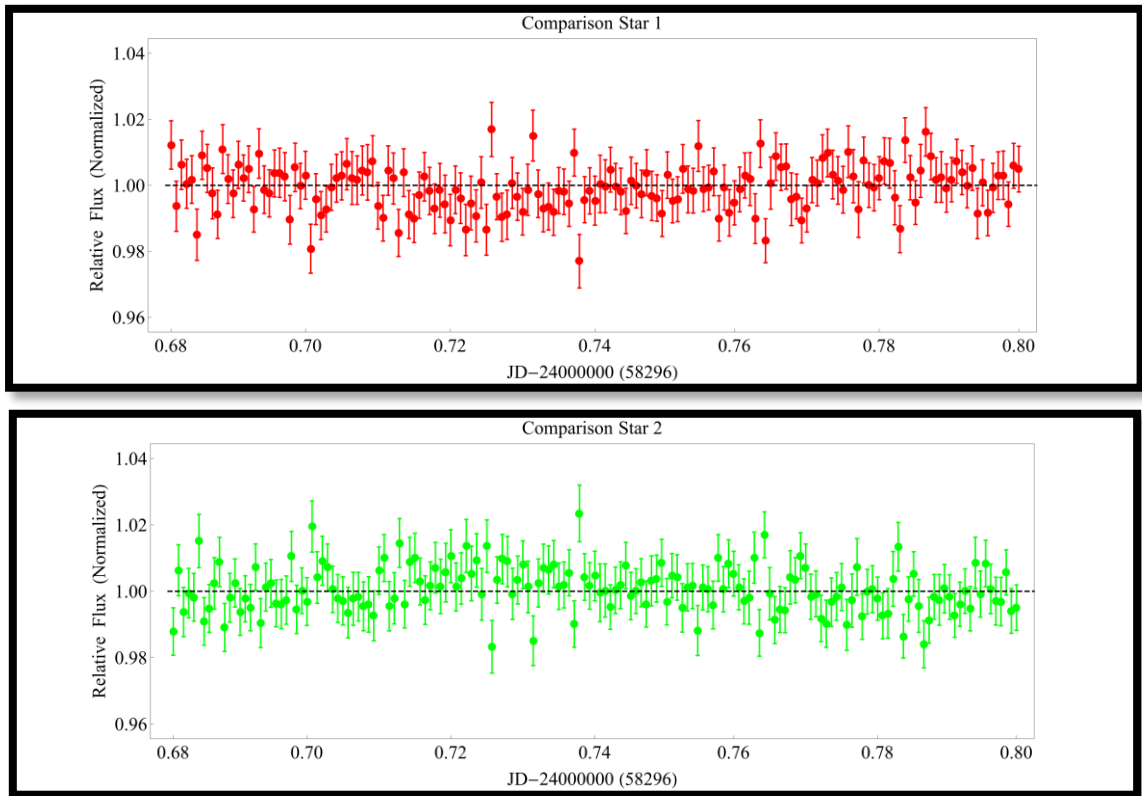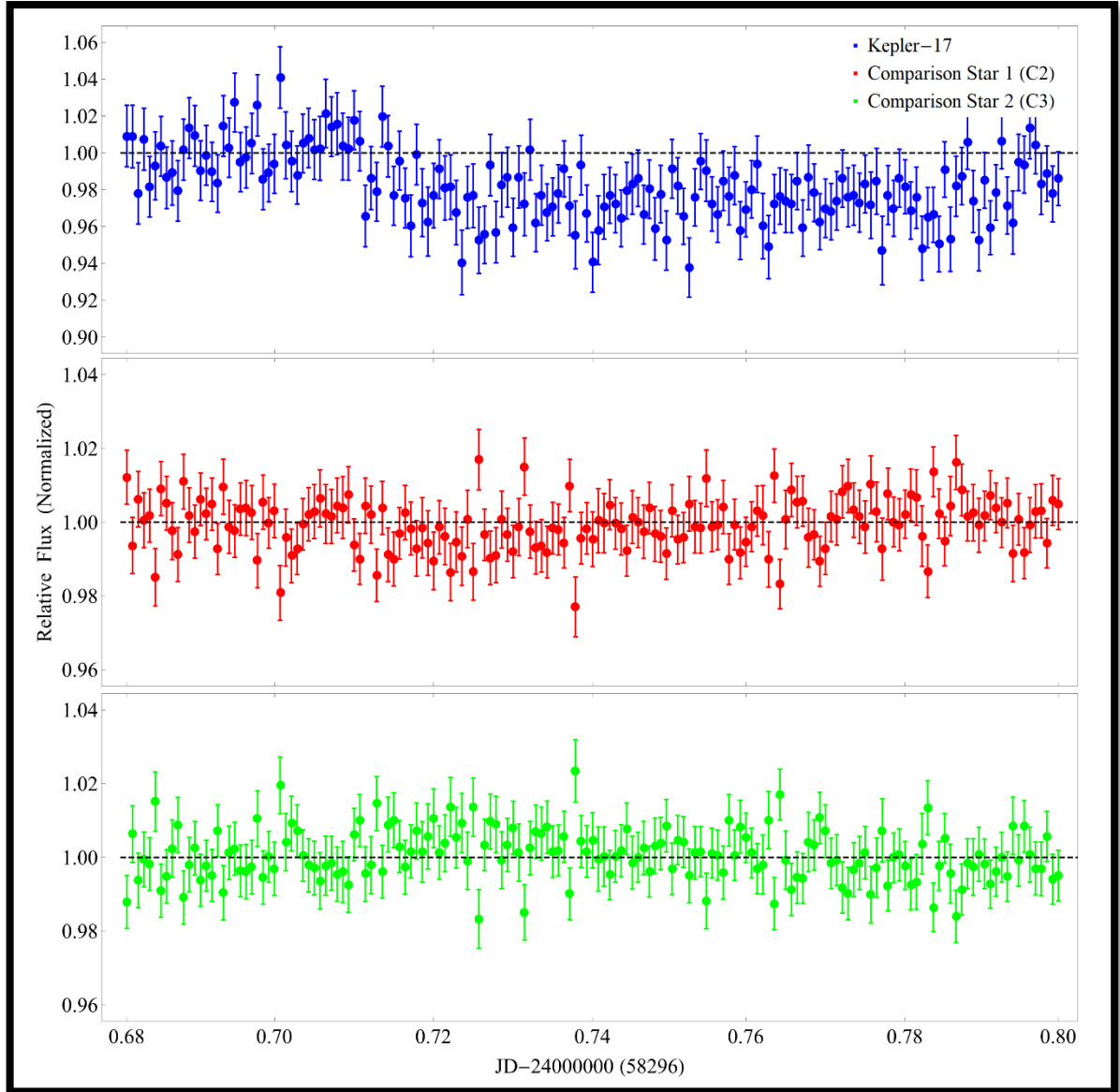

Figure 5: Normalized relative flux for comparison stars. Comparison star C2 is shown in red while comparison star C3 is shown in green.

---

[3] Note that this is an approximate model used for statistical purposes and that the normalized relative flux data contains non-Gaussian outliers and is correlated with the flux from the other measured stars.

host star magnitude. Thus, more stringent limits can be placed with reference stars of known magnitudes.

We took a random interval consisting of 30 consecutive mid-transit observations from the Kepler-17 light curve and found that 24 normalized relative flux values were lower than the 1.14% detection threshold. The probability of this occurring under a Gaussian white noise process is nearly zero.

With confidence in detection, one can begin to estimate planet parameters. However, complications towards the end of the transit with cloud obstruction limited planet parameter estimation capabilities by decreasing confidence in our estimates for the characteristic timescale values from Eqs. (4) and (5). Nevertheless, we were still able to obtain the estimates discussed in Sec. 2. The radius estimation was done using Eq. (1) and the host star radius stated in Sec. 3b. To calculate the peak brightness drop ΔL, we averaged consecutive normalized relative flux values corresponding to the middle of the transit (JD-2400000 times 58296.754 to 58296.760) and subtracted this mean from 1 (the pre-transit normalized relative flux). A planet radius of 1.555 R_{Jup} was calculated, overestimating the accepted value from Sec. 3b by 18.8%. We approximated the time of first contact by $t_1 = 58296.710$, the second contact with $t_2 = 58296.730$ and the third contact with $t_3 = 58296.790$. Since the fourth contact was not observed, we assumed the same time for ingress and egress and deduced a fourth contact time of $t_4 = 58296.810$. After establishing the characteristic time scales, we used the accepted inclination value of $i = 87.2°$ and calculated a planet semimajor axis of $a = 0.018$ au as well as a planet orbital period of 1.204 days. Table 1 outlines how these results compare to the accepted values.

Figure 6: Normalized relative flux for Kepler-17 (Blue) and the 4 comparison stars. The comparison star curves are shifted by a constant value and still retain their original shape.

Table 1: Kepler-17b Planet Parameter Estimation

Parameter	Units	Calculated	Accepted	% Error
Planet Radius R_{pl}	R_{Jup}	1.555	1.312	18.8 %
Semimajor Axis a	au	0.018	0.026	30.4 %
Orbital Period P	days	1.204	1.486	19.0 %

6 Discussion

With the observation of the Kepler-17b transit on June 26, 2018, we were the first to show the Great Basin Obsevatory's capability of extra-solar planet detection via transit photometry. Furthermore, we established a minimum transit depth threshold for which the GBO is capable of detecting an exoplanet transit with confidence. An adequate estimation of the exoplanet parameters was also achieved. Since our initial observations, exoplanets with brighter host stars have been detected using the GBO, such as the 11.06 magnitude star WASP-48, resulting in a radius estimation accurate to within 6% of the accepted value (see Ref. 5 for experiments to date). Future work will include observing the entirety of a transit as well as consecutive transits to obtain more confidence in establishing the characteristic time scales leading to more precise estimates for planet parameters. Moreover, the GBO is expected to be equipped with a spectrograph that can be used for exoplanet detection via the radial velocity method. This method will expand our exoplanet parameter estimation capabilities by allowing for planet mass approximations.

7 Acknowledgements

Appendix A - The Great Basin Observatory

The Great Basin Observatory (GBO) is the first research grade observatory ever built in a U.S. National Park. Set at an elevation of 6,825 feet, with no significant man-made light for 70 miles in all directions, the observatory is a state-of-the-art, remotely operated, optical astronomical telescope [5]. The creation of observatory has been a collaborative effort by the University of Nevada, Western Nevada College, Southern Utah University, Concordia University, and the Great Basin National Park Foundation.

The GBO enables researchers to explore fundamental questions about our universe. Its location in Great Basin National Park underscores the need to preserve night skies as a park resource.

The GBO's primary goals are to:

1. Inspire students and educators in the fields of astrophysics and other sciences, technology and natural resource management.
2. Provide a state-of-the-art research/education facility.
3. Preserve and utilize the spectacular dark night sky of Great Basin National Park.

References

1. Perryman, M. A. (2018). *The Exoplanet Handbook*. Cambridge: Cambridge University Press.

2. NASA Exoplanet Archive., https://exoplanetarchive.ipac.caltech.edu/

3. Carter, J. A., Yee, J. C., Eastman, J., Gaudi, B. S., & Winn, J. N. (2008). Analytic Approximations for Transit Light-Curve Observables, Uncertainties, and Covariances. *The Astrophysical Journal*, 689(1), 499-512. doi:10.1086/592321

4. Kepler-17. http://simbad.u-strasbg.fr/simbad/sim-id?Ident=Kepler-17

5. About The GBO. http://www.greatbasinobservatory.org/about-observatory